Indian Journal of Chemical Technology
Vol. 27, Nov 2020, pp. 441-451

Fabrication and characterization of composite (nano)polyaniline/polyimide membrane for pervaporative separation of 1-octene/benzene mixtures

Monalisha Samanta, Sayan Roychowdhury & Debarati Mitra*
Department of Chemical Technology, University of Calcutta, 92 Acharya Prafulla Chandra Road, Kolkata 700 009, India
E-mail: debarati.che@gmail.com

Received 13 May 2020; accepted 28 October 2020

The variation of modern separation technology of aromatics/aliphatics mixture is membrane process and development of new membrane materials (polymeric and composite) for high efficiency. Nano-polyaniline has been prepared by bulk polymerisation method and is used for the fabrication of (nano)polyaniline/polyimide ((nano)PANI/PI) composite membrane to achieve pervaporative separation of 1-octene/benzene mixture. Benzene is carcinogenic compound in group 1 of monograph of International Agency for Research on Cancer. Transmission electron microscopy confirmed the generation of (nano)PANI (particle size 8-9 nm). Both membrane and (nano)PANI have been characterised by Fourier transmission infra-red spectroscopy, Scanning electron microscopy, X-ray diffraction and Atomic force microscopy. The swelling behaviour and mechanical properties of the composite membrane are also investigated. Incorporation of (nano) PANI in the polyimide matrix increases the polarity of the membrane, thereby increasing its selectivity towards 1-octene. The highest permeation flux and separation factor achieved are13.88 $kg.m^{-2}h^{-1}$ and 6.44 respectively at 333 K and 1 mm Hg downstream pressure.

Keywords: 1-octene/benzene mixture, Nanocomposite membrane, Permeation flux, Pervaporation, Separation factor

Refineries as well as petrochemicals often require separation of aromatics/aliphatics mixtures in order to achieve the desired product quality and control environmental pollution[1-3]. Usually the main products of refineries are gasoline, diesel and lube oil. All products contain different aromatic compounds. Generally gasoline and diesel are used as automotive fuel. Both gasoline and diesel contain aromatics which are detrimental to human health. Most of them are carcinogenic in nature announced by IARC (International Agency for Research on Cancer) and EPA (Environmental Protection Agency)[4,5]. Hence, emission of aromatics along with the un-burnt hydrocarbons can adversely affect the environment. Recently, many countries have imposed limits on the presence of aromatics in fuel as adopted by EURO (European emission standards) and EPA regulations[6]. However, separation of aromatics/aliphatics mixtures is relatively difficult due to their close boiling points[7,8]. The conventional separation processes of these type of mixtures are azeotropic distillation, extractive distillation etc. These processes are quite expensive and complicated[9,10]. Membrane separation techniques might serve as a promising alternative. Among different membrane separation processes, pervaporation (PV) is a useful analytical tool that features simplicity, reduced energy consumption, automation and cleanliness. PV technology is a unique membrane separation process combining permeation and evaporation. The separation mechanism in this process is based on the difference in sorption and diffusion (properties) through the membrane of the permeating components. The upstream side of the membrane is at ambient pressure while the downstream side is either under high vacuum or purged with an inert gas that allows evaporation of the selective component after permeation through the membrane[11-13]. The PV efficiency is evaluated in terms of permeation flux, membrane selectivity/separation factor/enrichment factor. This efficiency is highly dependent on membrane material/composition. As evident from literature, for separation of aromatics/aliphatics mixture, the most useful membrane materials include aromatic-polyimides, polyurethanes, poly (ether amide)s, polyacrylates, poly (methyl methacrylate)s and poly (ether-block-amide)[14-22]. Polyimide (PI) is an excellent polymer to prepare pervaporative membranes because it is both mechanically and thermally stable, as observed by Vanherck *et al*.[23]. It is also chemically inert in different solvents[23]. Many

aromatics/aliphatics like benzene/cyclohexane, toluene/n-heptane, benzene/*n*-heptane, naphthalene/*n*-decane mixtures were separated using PI based membrane using PV technique yielding high permeation flux[8,14,24-26]. Nanocomposite pervaporative membranes have been fabricated by incorporating organic or inorganic nanoparticles (NPs) into polymeric/ceramic membrane matrix to achieve high separation efficiency and improving the anti-fouling character for aromatics/aliphatics separation[27-31]. The previous researchers have used different types of organic NPs such as grapheme oxide (GO), carbon nanotube (CNTs), polyaniline (PANI) etc, inorganic NPs like zinc oxide (ZnO), silver (Ag), silicon di-oxide (SiO_2), etc. to form composite or mixed matrix membranes (MMMs)[29,30]. Dai *et al*.[27] prepared a nanocomposite membrane by impregnation of GO/NPs-Ag (15 mass %) into PI matrix to separate benzene/cyclohexane. They observed that GO-Ag/PI hybrid membrane had 3 times greater separation factor than GO/PI membrane.

Nano-PANI is an important blending material for preparation of a composite polymeric membrane due to its easy oxidative polymerisation, high yield with low cost, high surface area, small diameter and extremely porous nature[31-33]. PANI particles have good practical impact due to their high electrical conductivity, high thermal as well as chemical stability. It is an air stable polar polymer that can be used to prepare the composite membranes with good transport properties[34]. Polotskaya and co-workers prepared a nano-composite membrane by incorporating nano-sphere-PANI (6 wt %) into the matrix of PI for the separation of methanol-toluene and methanol-cyclohexane mixtures. They found that the PI/PANI composite membrane had 1.5 times greater efficiency than simple PI membrane[35].

In this research work, a unique (nano)PANI/PI composite membrane was synthesized. The synthesized membranes as well as nano-PANI particles were characterized by FTIR (Fourier transmission infra-red spectroscopy), SEM (Scanning Electron Microscopy), AFM (Atomic Force Microscopy) and XRD (X-ray diffraction). The mechanical strength and swelling study of the composite membrane were also carried out. The composite membrane was utilised to separate the 1-octene/benzene mixture using PV technique and the membrane efficiency was estimated in terms of flux and selectivity.

Experimental Section

Materials

Polyamic acid (dissolved in toluene) and dioctyl sebacate (assay ≥97.0%) were purchased for fabrication of the membrane and also 1-octene (assay ≥97.0%) as well as benzene (assay ≥99.0%) were purchased for preparation of feed mixture, from Sigma Aldrich. Aniline (Purity ≥99.5%), ammonium persulfate (APS) (assay≥98%), N-methyl-2-pyrrolidone (NMP) (assay ≥99.5%), and concentrated hydrochloric acid (HCl) (assay ≥37%) were bought from Merck Life Science Pvt. Ltd., Mumbai for synthesis of PANI.

PANI preparation

Solution (A) was prepared by mixing 4.5 g aniline with 50 mL 1(M) HCl acid. Then 12 g APS was dissolved in 50 ml distilled water to prepare solution (B). These two solutions were mixed together and stirred uniformly for 24 h at 273 K. A dark green coloured precipitate was formed. The precipitate was filtered and dried at 333 K for 24 h to get a dark green powder of PANI salt. The green powder was then washed with ammonium hydroxide and a blue precipitate was formed. This blue precipitate was also filtered and dried at 333 K for 24 h to obtain the blue powder of PANI base which was later added to the membrane casting solution[33,35]. The preparation of PANI is represented in Fig. 1.

Membrane preparation

0.05 weight % of PANI was mixed with polyamic acid (dissolved in toluene) and stirred for 4 h at 298 K to prepare the membrane casting solution. This solution was casted on a glass plate by using a scraper and the casted film was dried at 320 K for 45 minutes in a vacuum oven for evaporation of the solvent. After that, for gelation the partially dry casting layer was kept immersed in dioctyl sebaceate for 12 h. Then the film was imidized at 323 K and 373 K in a muffle furnace for 1 h respectively. Finally, the membrane was washed with methanol and distilled water and dried at 333 K for 30 minutes in a vacuum oven and the composite membrane was formed[12,34].

Membrane thickness

The thickness of the composite membrane was measured by using Yuzuki digital micrometer, Mumbai, India. This estimation was done by measuring the thickness at 6 different positions of the membrane. The average thickness was calculated.

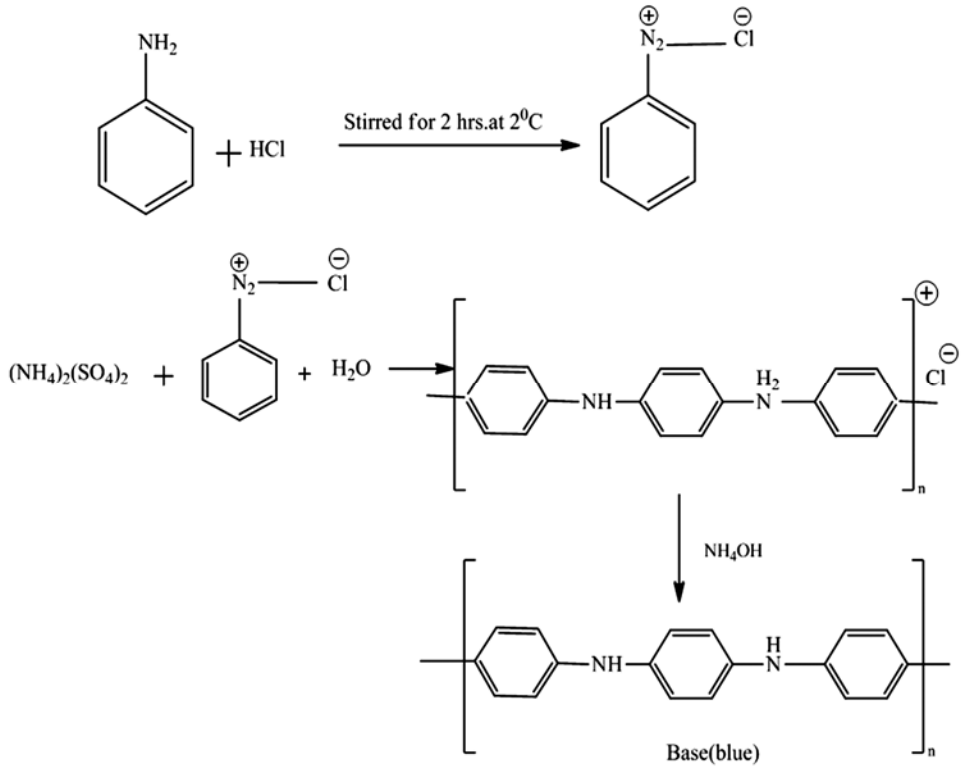

Fig. 1 — Preparation of PANI

Characterisation of PANI/PI membrane

Mechanical properties

The tensile strength of the virgin composite membrane and worked membrane were analysed by universal testing machine ZWICK ROELL Z010. The virgin composite membrane and worked membrane after 30 experimental runs were cut into standard dimension (20 mm length and 5 mm width). These cut membranes were clamped at both ends and the speed of elongation rate was 20 mm/min. The values of tensile strength, Young's modulus and stiffness of the membrane were determined.

Sorption test

Approx 0.5 g of membrane strips were weighed and then dipped into different mixtures of benzene and 1-octene for the determination of gravimetric sorption test i,e interaction of the mixture and the membrane. The sorption test was done at 303 K. The membrane strips were taken out from mixture and excess solvent was removed from the surfaces using tissue paper. Without any delay, the strips were weighed. From the sorption test, percentage of swelling was calculated from this following equation[36],

$$\% \text{ swelling} = \frac{S_M - D_M}{D_M} \times 100 \quad \ldots (1)$$

where, S_M denotes the weight of Swelled membrane and D_M represents the weight of dry membrane.

Structural characterisation of PANI and (nano)PANI/ PI membrane

Ultraviolet Visible spectroscopy (UV-Vis)

The UV-Vis absorption peak of PANI was analysed by double beam SHIMADZU 1800 UV spectrometer (Japan) at 298K with a scanning range from 300 to 800 nm.

Transmission emission microscopy (TEM)

The size of PANI powder was analysed by TEM using JEOL JEM 2100HR with EELS, USA. Before TEM experiment, dilute PANI solution (50 ppm of PANI powder dissolved in NMP) was prepared. This solution was dropped on a copper grid. After 12 h, the copper grid was placed in the instrument for analysis.

Scanning electron microscopy (SEM)

The surface morphology of the PANI was studied by SEM, equipped with Ion Sputter E1010, (ZEISS

EVO18) Germany. The surface as well as cross section of prepared virgin composite membrane and worked after 30 experimental runs of same membrane were analysed by using same scanning microscope. PANI and membrane were silver coated with sputter coater before conducting the SEM.

Atomic force microscopy (AFM)

The surface roughness of PANI powder and (nano)PANI/PI membrane were analyzed by AFM using 5500 Atomic force microscope (N9410A, USA). Before analysis, PANI powder was dissolved into NMP to get a transparent film on a cover slip. The cover slip of PANI and (nano)PANI/PI membrane were placed on glass slides with the help of silver coating.

Fourier transformation infrared spectroscopy (FTIR)

The functional groups of PANI was analysed using NICOLET 6700 FT-IR Spectrometer, USA**.** Before the experiment, PANI powder was intimately ground with pure potassium bromide (KBr) in a mortar pestle and using hydraulic pressure a thin pellet was formed which was placed in FTIR beam for analysis. The functional groups of membrane were also analyzed with the help of the FTIR in attenuated total reflection (ATR) mode. The spectrum range applied was 4000–600 cm^{-1}.

X-ray diffraction (XRD)

The crystalline structure of PANI and intermolecular distance between the intersegment chains of (nano)PANI/PI membranes were determined by XRD using Panalytical X'Pert Pro XRD (PW 3040/60, Netherland) through Cu/Kα radiation. The wavelength of the X-rays used was 1.54 . The 2θ range of X-ray was 10° to 60° at a scanning rate of 0.01°/sec.

Pervaporation experiments

Benzene and 1-Octene mixture was separated through PV using (nano)PANI/PI membrane. The PV experiment was carried out in a batch set up in laboratory scale. The PV set up was build with a stainless steel permeation cell, agitator, heater, temperature sensor, cold (liquid nitrogen contain) trap for collection of permeate, vacuum pump for downstream pressure. The (nano)PANI/PI membrane was placed on porous metal support. The operational membrane area was 39.69 $\times 10^{-4}$ m^2. The operating temperature was varied from 298 K to 343 K with 1 mm Hg downstream pressure. The permeation flux for binary system is represented by the following equation[37],

$$J = \frac{Q}{At} \quad \ldots (2)$$

where, J represents the permeation flux ($kg.m^{-2}h^{-1}$), Q represents the total mass (g) of permeate collected, A denotes the effective area of membrane (m^2), t is operational time (h)

The separation factor (β_{AB}) of PV process for binary system[38],

$$\beta_{AB} = \frac{P_A / P_B}{F_A / F_B} \quad \ldots (3)$$

where, P_A is mass (g) of component A in permeate, P_B is mass (g) of component B in permeate, F_A is mass (g) of component A in Feed, F_B is mass (g) of component B in Feed

Here, A represents 1-Octene and B represents Benzene

Activation energy

Arrhenius' equation represents the relationship between absolute temperature (T) and permeation flux (J)[39],

$$J = J_O \exp\left(-\frac{E_a}{RT}\right) \quad \ldots (4)$$

$$\text{or, } \ln J = \ln J_O - \frac{E_a}{RT} \quad \ldots (4a)$$

where, E_a is the activation energy (KJ/mol), J_0 is the pre-exponential factor ($mol.m^{-2}.h^{-1}$), R is universal gas constant ($J.mol^{-1}.K^{-1}$) and T is absolute temperature (K).

Analysis by Gas Chromatography (GC)

The components in permeate and retentate were analysed by GC TRACE 1300, Thermo Fisher Scientific, USA. The TR-5 GC column was used and internal diameter and thickness of this column was 30 m × 0.32 m and 1×10^{-2} mm respectively. Here, the flow rate of carrier gas (nitrogen) was 1.5 mL/min. The oven temperature was programmed between 313 K and 404 K. In this system, Flame ionization detector (FID) was used and it's temperature was maintained at 423K. The oven run time was 11.5 minute. The operation was done in split flow mode with 50 ml/min and the split ratio was 33.3.

Results and Discussion

Physical appearance of membrane

The surface of (nano)PANI/PI composite membrane appeared smooth in naked eye. This polymeric composite membrane is greenish yellow in colour because of the dark green colour of PANI incorporated into the PI matrix. The average thickness of this PANI/PI composite membrane is 0.32 mm.

Mechanical property

The mechanical properties of virgin (nano)PANI/PI membrane and used membrane were studied in terms of tensile strength, Young's modulus and stiffness. After 30 PV experiments the strength of the membrane was somewhat less than the virgin membrane probably due to degradation of membrane by swelling[40]. Table 1 represents the mechanical strength of (nano)PANI/PI composite membrane. From Table 1, it is evident that the composite is a thermosetting polymer due to its high stiffness and Young's modulus and it cannot be re-melted[41].

Structural Characterisation of PANI and PANI/PI membrane

TEM of PANI

The size of the PANI nanoparticles was estimated by using TEM (Fig. 2A) and was found to be 8 to 9 nm.

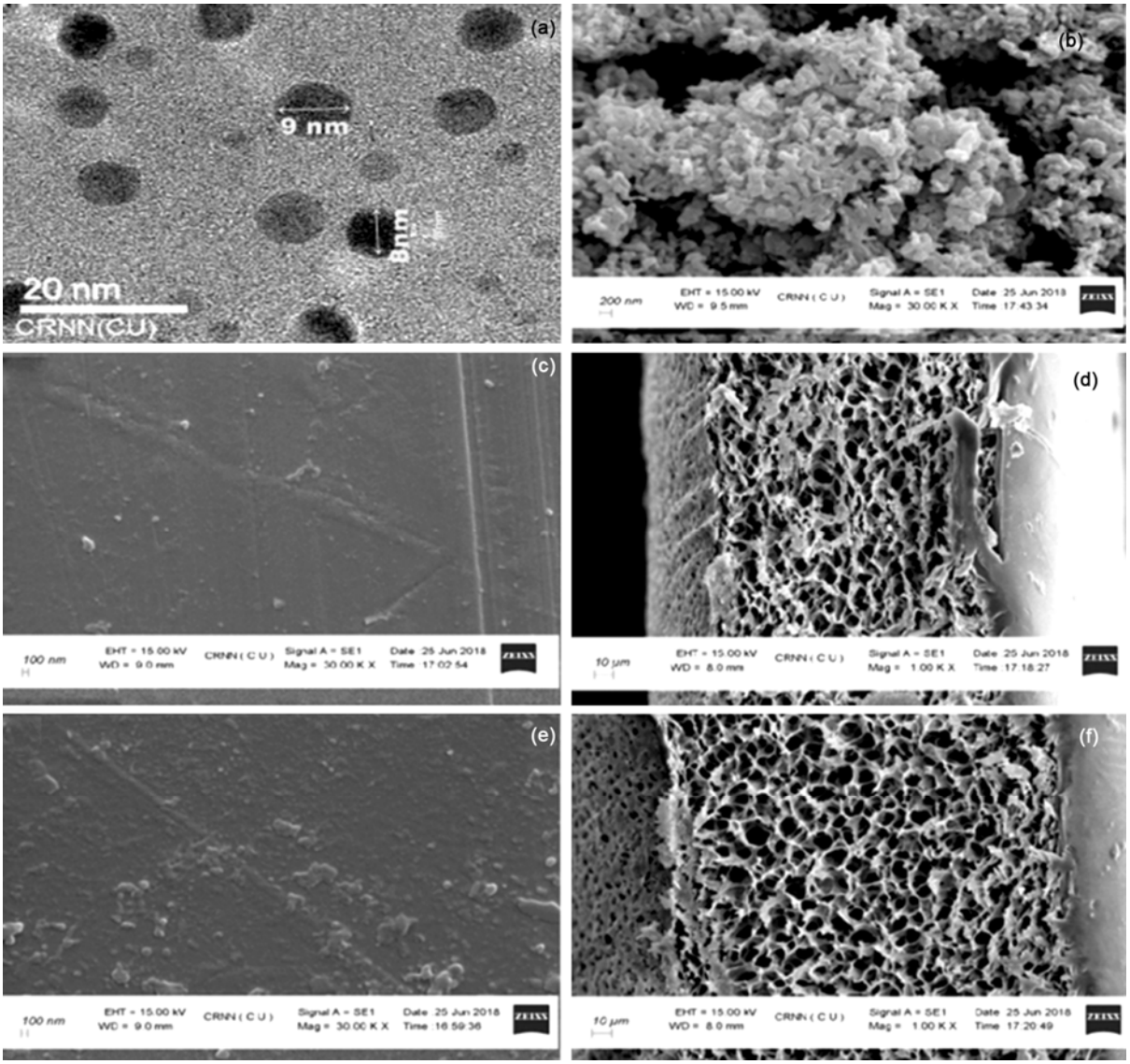

Fig. 2 — Electronic microscopic image Fig. 3A,TEM of PANI Fig. 3B, SEM of PANI Fig. 3C, SEM of virgin (nano) PANI/PI composite membrane Fig. 3D, Cross-section image of virgin (nano) PANI/PI composite membrane Fig. 3E, SEM of used (nano) PANI/PI composite membrane Fig. 3F, Cross-section image of used (nano) PANI/PI composite membrane

SEM of PANI and (nano)PANI/PI membrane

The size of PANI was analyzed using SEM. The average size of the PANI particles is approximately 95 nm from the SEM image shown in Fig. 2B. The particle size of PANI established from TEM is however smaller than that observed in SEM, due to higher resolution of TEM[42]. The surface morphological structure and cross-section of virgin and used (after 30 experiment runs) membranes were analyzed by SEM shown in (Figs. 2C, 2D, 2E and 2F). It is quite clear that the surface of virgin membrane is smoother than the used membrane perhaps due to swelling by 1-octene/benzene mixture during PV experiments. From the cross-sectional image (Figs. 2D and 2F) of virgin and used membranes, it is evident that the top layer of these membranes is dense underneath of which lies a spongy layer probably due to the incorporation of nano-PANI which is a porous material and has large surface area[35]. It can also be inferred that PANI has been well-distributed in the PI matrix to form a composite membrane.

Table 1 — Mechanical strength of (nano) PANI/PI composite membrane

Sample	Tensile strength (MPa)	Stiffness (N/M)	Young's Modulus (MPa)
Virgin(nano)PANI/PI Membrane	11.65	9677.68	155.55
Used(nano)PANI/PI Membrane	10.14	9404.35	143.90

AFM of PANI, PI and (nano)PANI/PI membrane

The roughness (Ra) of PANI, PI membrane and both virgin and used (nano)PANI/PI composite membranes were estimated by the three dimensional images of AFM. The roughness of PANI, PI membrane, the virgin as well as the used composite membranes is 5.35 nm, 11.10 nm, 5.55 nm and 5.85 nm respectively. The surface of PANI and all the membranes are almost smooth from the observed AFM images (Fig.3). Fig. 3G represents the 3D image of used composite (after 30 runs) membrane. The roughness of this membrane is slightly higher than the virgin membrane probably from swelling.

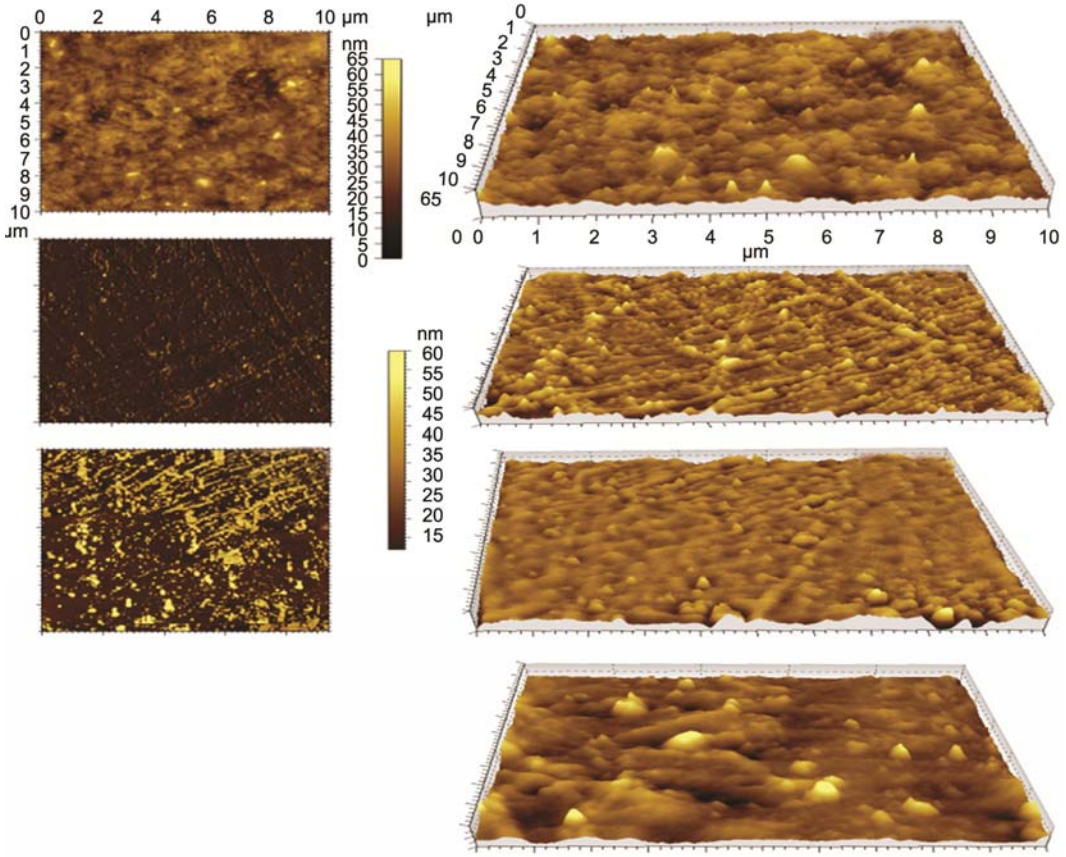

Fig. 3 — AFM image Fig. 4A, 2D phase image of PANI Fig. 4B, 3D image of PANI Fig. 4C, 2D phase image of PI membrane Fig. 4D, 3D image of PI membrane Fig. 4E, 2D phase image of virgin (nano)PANI/PI composite membrane Fig. 4F, 3D image of virgin (nano)PANI/PI composite membrane Fig. 4G, 3D image of used (nano)PANI/PI composite membrane

The Fig. 3A, 3C and 3E represent the 2D phase images of PANI, PI membrane and composite membrane. From AFM 2D phase image, it is clear that the composite membrane has two phases while the PI membrane and PANI both have a single phase[43,44].

FTIR of PANI PI, and (nano)PANI/PI membrane

The FTIR of PANI particles, PI membrane and nanocomposite membrane are shown in Fig. 4 in the range 4000 to 600 cm^{-1}. The peaks of PANI and (nano)PANI/PI membrane are similar due to the presence of PANI[35]. The characteristic peak of (nano)PANI/PI membrane observed at 3128 cm^{-1} is for N-H stretching. Peaks for N-H stretching are observed at 3230 cm^{-1} and at 3089 cm^{-1} for PANI and PI membranes respectively. The strongest peak of C=O symmetric stretching for PI membrane and (nano)PANI/PI composite membrane is present at 1720 cm^{-1} and 1715.6 cm^{-1} respectively[35,40]. But in case of composite membrane, the symmetric stretching of C=O has slightly shifted (4.4 unit) probably due to interaction of PI and (nano)PANI. It may also be concluded that a minor weak hydrogen bond formation between carbonyl group of PI and imide group of PANI[34,35] has occurred. The C-N stretching of PI membrane, (nano)PANI/PI membrane and PANI is present at 1380 cm^{-1}, 1368 cm^{-1} and 1307 cm^{-1} respectively and aromatics rings vibration for PI membrane and (nano)PANI/PI composite membrane is evident from the peaks at 1287 cm^{-1} and 1236 cm^{-1} respectively. Here also both C-N stretching and the aromatics rings vibrations have shifted slightly probably because of interaction between phenyl rings of PANI and PI[34]. The main distinguishable peaks of PANI at 1589 cm^{-1} and 1498 cm^{-1} are for quinonoid (Q) and benzenoid (N) rings of C-C bond stretching respectively[32]. The benzenoid (N) stretching of PI membrane and (nano)PANI/PI is present at 1495 cm^{-1} and 1498 cm^{-1} respectively. From the Fig. 4, N-Q-N stretching for (nano)PANI/PI membrane is represented at 1500 cm^{-1}. It may be concluded that the shifts in bond stretching may be attributed to the interaction of π donor of PANI and π acceptor of PI or due to H- bonding of amino groups (N-H) of PANI and carbonyl groups (C=O) of PI.

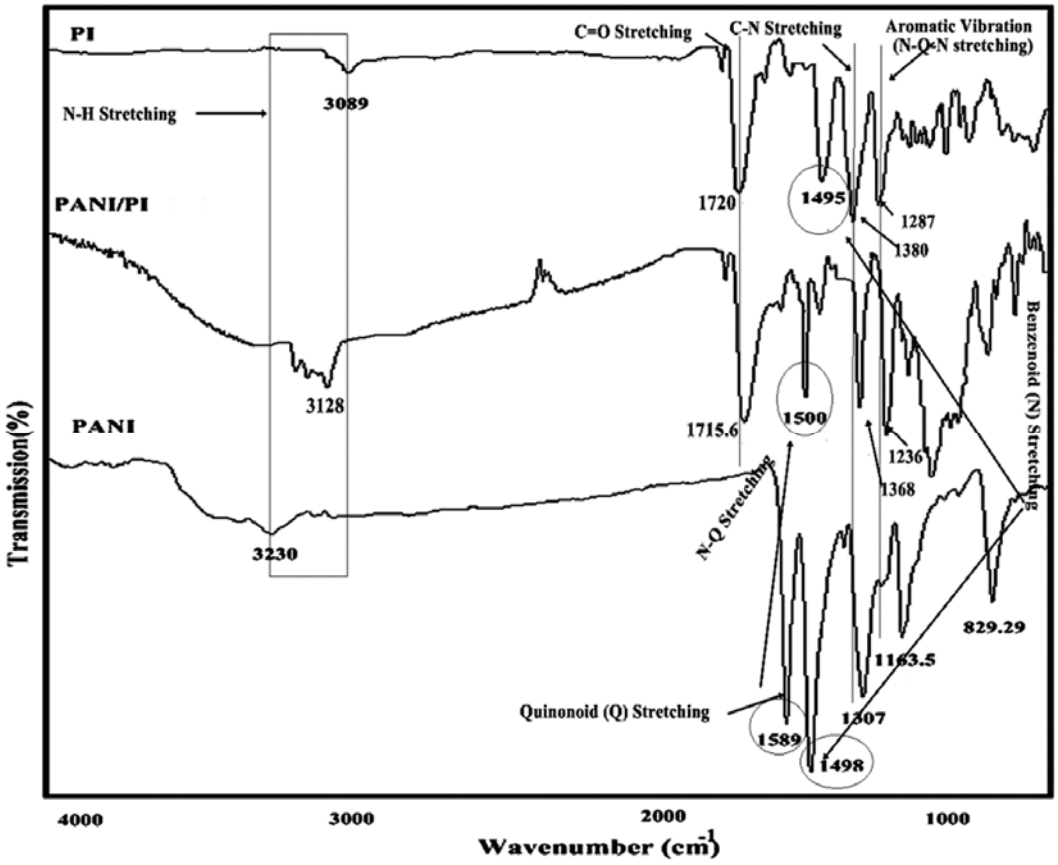

Fig. 4 — FTIR of PANI, PI membrane and (nano)PANI/PI composite membrane

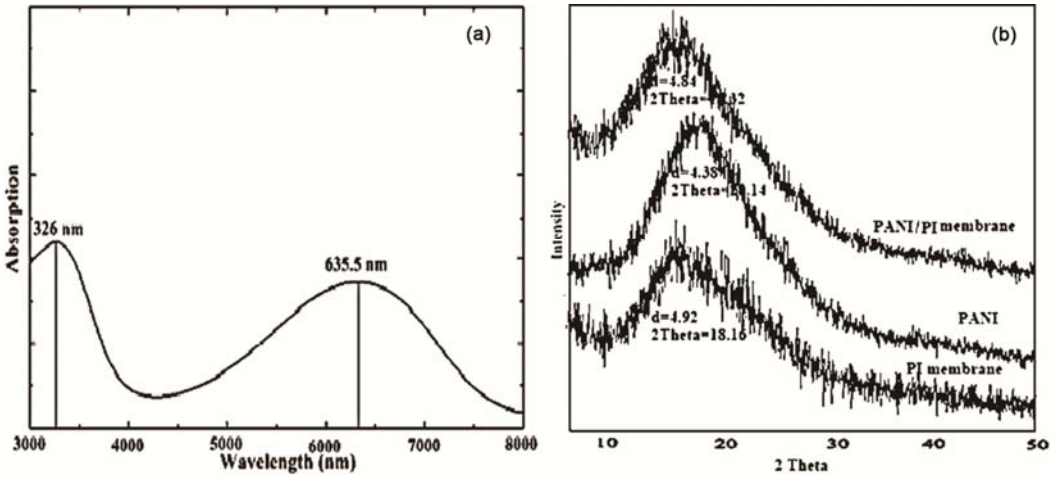

Fig. 5 — (A) UV of PANI, (B) XRD of PI membrane, PANI and (nano)PANI/PI composite membrane

UV-Vis of PANI

The UV-Vis transmission curve was analysed for the characterisation of PANI base or salt. The two characteristic absorption peaks of PANI are observed (Fig. 5A) at 327 nm and 635.5 nm. The 327 nm peak represents the π-π* transmission of benzenoid ring of PANI base. Another peak 635.5 nm is characteristic of the quinonoid ring of PANI base[35]. So, it may be concluded that the UV-Vis transmission plays a supporting role for the FTIR peaks of PANI.

XRD of PANI, PI and (nano)PANI/PI membrane

The crystallography of PANI powder, PI and (nano)PANI/PI composite membranes were studied by XRD. From Fig. 5B it has been revealed that the PANI powder is primarily amorphous in nature. The (nano)PANI/PI membrane is also amorphous. In this figure, the 2θ of PANI is 20.14° whereas the 2θ of PI is 18.16°. PANI particles are incorporated into the PI membrane. For this reason, it may be concluded that 2θ of (nano)PANI/PI composite membrane is 18.32° [32,35]. The d spacing and FWHM (β) of PANI are 4.38Å and 1.66 respectively. Using XRD data, the crystal size of PANI is calculated with the help of Scherer equation[35] that is 8.43 nm in coherence with TEM of PANI.

Performance study of (nano)PANI/PI membrane

Swelling analysis

Percentage of swelling was analyzed to study the interaction of the composite membrane with benzene and 1-octene. Polotskaya *et al*.[34] observed that this type of composite membrane has less affinity towards aromatic compounds. The swelling analysis of the composite membrane is done by plotting % of swelling

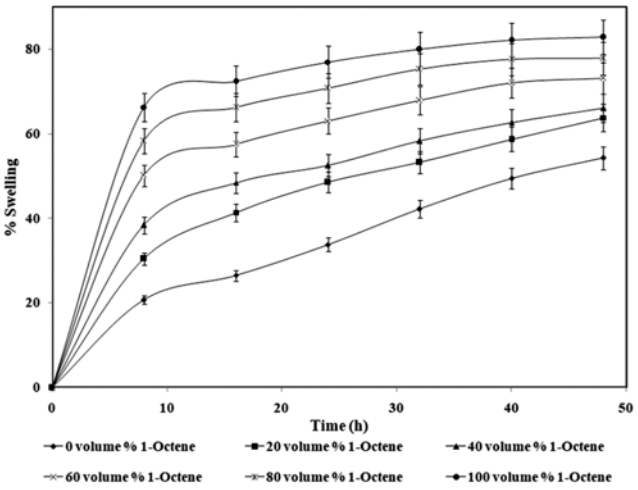

Fig. 6 — Swelling behavior of (nano)PANI/PI composite membrane

vs time intervals for different volume percentage of benzene in feed mixture at temperature 303 K (Fig. 6). When 1-octene is present in feed mixture (100%) then the membrane achieves equilibrium swelling at about 40 h, whereas, for 100% benzene, the membrane swelling increases even beyond 48 h. Thus, when lower percentage of benzene is present in feed mixture then the equilibrium swelling of membrane is observed to reach faster. From swelling data, it is evident that the membrane has greater affinity for 1-octene than benzene. Presence of polar nano-PANI (dipole moment = 6.978D)[45] results in greater interaction between the membrane and 1-octene (dipole moment =0.39D)[46] rather than with benzene (dipole moment =0.0001D)[46]. Thus swelling data indicates that the synthesized membrane will allow 1-octene to permeate in preference to benzene.

Determination of Activation energy

The activation energies of permeation of 1-octene and benzene are calculated from the plot of lnJ vs 1/T (Fig. 7). The calculated activation energy of permeation and pre-exponential factor for 1-octene and benzene is given in Table 2.

Calculation of Permeation Flux (J) and Separation Factor (β)

The permeation flux as well as separation factor of the composite membrane for 1-octene/benzene mixture were calculated after PV experiments. From Fig. 8, it is evident that the total permeation flux increases with increasing temperature and fixed downstream pressure (1 mm Hg) as a function of concentration of 1-octene in feed mixture, reaches a maximum value at about 333K and then levels of. Similar behavior has been reported by previous researchers[12,17,40,47]. The activation energy of permeation is positive (Table 2) which also indicates permeation flux is expected to increase with increasing temperature. The enhancement of total permeation flux with temperature may also be attributed to the increase in the mobility of the polymeric chains[48] thereby creating free volumes of the polyimide base membrane that results in greater rate of diffusion of the permeating species through the membrane[49].

Table 2 — Calculation of activation energy

Feed component	E_a (KJ/mol)	J_O (mol/m^2/h	R^2
1-Octene	2.4	4.25	0.978
Benzene	4.6	4.61	0.964

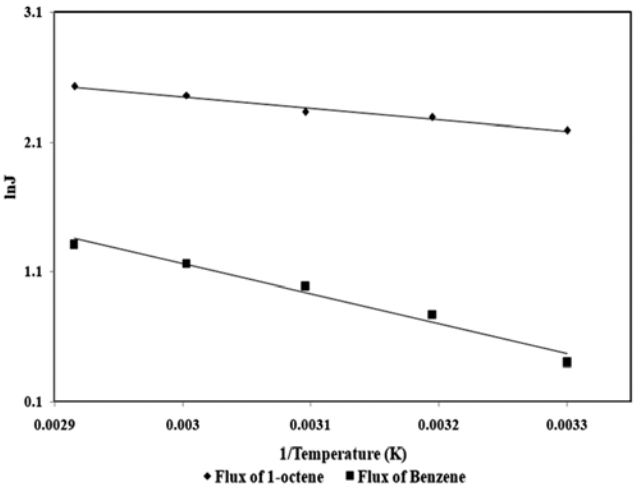

Fig. 7 — Relation between lnJ and 1/Temperature

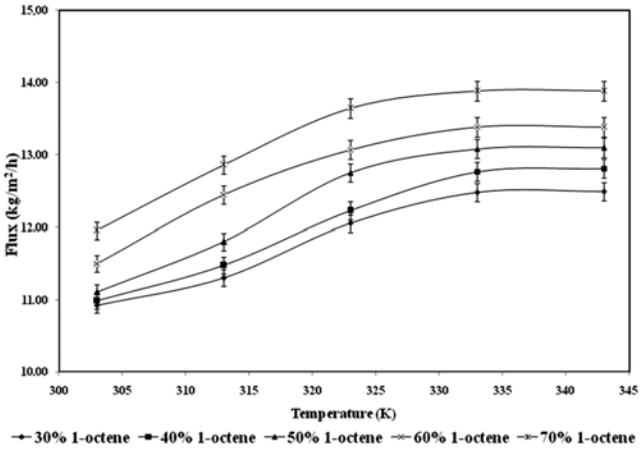

Fig. 8 — Flux of (nano)PANI/PI composite membrane for different concentration of 1-octene/benzene mixture at different temperature at 1 mm Hg of downstream pressure

The separation factor also increases with increasing temperature till 333K for all feed mixtures. The driving force for the separation of any mixture using PV technique is due to the difference in chemical potential gradient of the feed components in terms of solubility and diffusivity between the feed and permeate sides based on the solution-diffusion theory[50,51]. Due to the linear structure and lower kinetic diameter of 1-octene (< 5.0 nm)[52] than benzene (5.85 nm)[53] rate of diffusion of the former molecules are expected to be faster than the latter; also resulting in an enhancement in the value of the separation factor with temperature (higher rate of diffusion at higher temperature) and downstream pressure of 1 mm of Hg (Fig. 9). Again, activation energy of 1-octene (2.4 KJ/mol) is lower than that of benzene (4.6 KJ/mol). So, 1-octene is expected to preferably permeate through this membrane. However, after 333K there is no appreciable increase

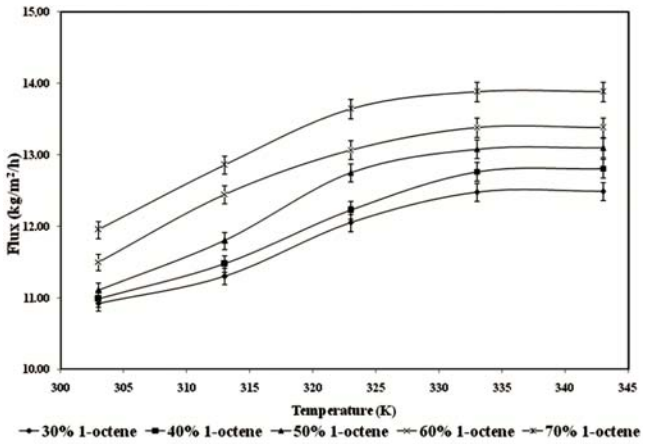

Fig. 9 — Separation factor of (nano)PANI/PI composite membrane for different concentration of 1-octene/benzene mixture at different temperature at 1 mm Hg of downstream pressure

in separation factor for all feed compositions. However, for feeds containing more than 60% by volume of 1-octene, the separation factor decreases probably due to simultaneous diffusion of both the permeating species through the highly swelled membrane.

Conclusions

In petroleum industries, separation of close boiling aromatics/aliphatics mixtures often poses a challenge to refiners. In this study, PANI/PI nanocomposite durable membrane was synthesized using a relatively simple method and characterized by SEM, FTIR, AFM, mechanical study and sorption study and utilized for the separation of 1-octene/benzene mixture applying PV technique. From the characterization study, it may be inferred that this membrane is dense, has greater affinity towards 1-octene and is mechanically stable. The highest permeation flux achieved is 13.88 $kg.m^{-2}.h^{-1}$ for 70 volume % of 1-octene in feed at 333 K and 1 mm of Hg downstream pressure. The maximum value of the separation factor for the system under investigation is 6.44 at 333 K and 1 mm of Hg for 60 volume % of 1-octene in 1-octene/benzene mixture. So, it may be concluded that PV operation using the fabricated membrane can be successfully applied for the separation of the chosen mixture.

Acknowledgement

The authors acknowledge the Central Research Facility (CRF) in IIT Kharagpur, India and the Centre for Research in Nanoscience and Nanotechnology in University of Calcutta, India for giving analysis facility. They are also thankful to departmental DRS I program under UGC, SAP, Government of India (Sanction No. F.5-9/2016/DRS-I(SAP-II) for providing partial financial support.

Conflict Of Interest

Authors declare that there is no conflict of interest regarding this publication.

References

1 Khazaei A, Mohebbi V, Behbahani R M & Ramazani A S A, *J Appl Polym Sci*, 135 (2018) 45853.
2 Diestel L, Bux H, Wachsmuth D & Caro *J, Micropor Mesopor Mat*, 164 (2012) 288.
3 Bahmanyar M, Sedaghat S, Ramazani S A & Baniasadi H, *Polym Plast Technol Eng*, 54 (2015) 218.
4 Benzene-EPA (Environmental Protection Agency, USA) 2016
5 Benbrahim-Tallaa L, Baan R A, Grosse Y, Lauby-Secretan B, El Ghissassi F, Bouvard V, Guha N, Loomis D & Straif K, *The Lancet Oncology*, 13 (2012) 663.
6 Aouinti L , Roizard D & Belbachir M, *Sep Purif Technol*, 147 (2015) 51.
7 Wang N, Wu T, Wang L, Li X, Zhao C, Jie L & Ji S, *Sep Purif Technol*, 179 (2017) 225.
8 Ribeiroa C P, Freemana B D, Kalikab D S & Kalakkunnath S, *J Membr Sci*, 390 (2012) 182.
9 Kononova S V, Kremnev R V, Suvorova E I, Baklagina Y G, Volchek B Z, Uchytil P, Shabsels B M, Romashkova K A, Setnickova K & Reznickova J, *J Membr Sci*, 477 (2015) 14.
10 Wu T, Wang N, Li J, Wang L, Zhang W, Zhang G & Ji S, *J Membr Sci*, 486 (2015) 1.
11 Nath K, *Membrane Separation Processes* (Easter Economy Edition. PHI Learning Pvt.ltd., India), 2012, 200.
12 Samanta M, Roychowdhury S & Mitra D, *J Indian Chem Soc*, 95 (2018) 1003.
13 Thang H V & Kaliaguine S, *Chem Rev*, 113 (2013) 4980.
14 Ribeiroa C P, Freemana B D, Kalikab D S & Kalakkunnath S, *Ind Eng Chem Res*, 52 (2013) 8906.
15 Xu W, Paul D & Koros W, *J Membr Sci*, 219 (2003) 89.
16 Cunha V, Paredes M, Borges C, Habert A & Nobrega R , *J Membr Sci*, 206 (2002) 277.
17 Samanta M, Roychowdhury S & Mitra D, *Chem Pap*, 72 (2018) 3141.
18 An Q, Qian J, Zhao Q & Gao C, *J Membr Sci*, 313 (2008) 60.
19 Sun H, Lu L, Peng F, Wu H & Jiang Z, *Sep Purif Technol*, 52 (2006) 203.
20 Peng F, Jiang Z, Hu C, Wang Y, Lu L & Wu H, *Desalination*, 193 (2006) 182.
21 Wang N, Ji S, Li J, Zhang R & Zhang G, *J Membr Sci*, 455 (2014) 113.
22 Aouinti L, Roizard D, Hu G, Thomas F & Belbachir M, *Desalination*, 241(2009) 174.
23 Vanherck K, Koeckelberghs G, Vankelecom I F G, *Prog Polym Sc*, 38 (2013) 874.
24 Xu G F & Zhu W P, *Chinese J Polym Sci*, 29 (2011) 288.
25 Maji S & Banerjee S, *J Membr Sci*, 360 (2010) 380.
26 Maji S & Banerjee S, *J Membr Sci*, 349 (2010) 145.
27 Dai S Q, Jiang Y Y, Wang T, Wu L G, Yu X Y, Lin J Z & Shi S X X, *J Colloid Interface Sci*, 478 (2016)145.
28 Goh P S, Ismail A F, Sanip S M, Ng B C & Aziz M, *Sep Purif Technol*, 81 (2011) 243.
29 Jhaveri J H & Murthy Z V P, *Desalin Water Treat*, 57 (2016) 26803.
30 Roy S & Singha N R, *Membranes*, 7 (2017) 53.
31 Neelgund G M & Oki A, *Polym Int*, 60 (2011) 1291.
32 Chen D, Miao Y E, Liu T, *ACS Appl Mater Interfaces,* 5(4) (2013)1206.
33 Rohani R, Yusoff I I, Efdi F A M & Junaidi M U M, *J Kejuruter*, 29 (2017) 121.
34 Polotskaya G A, Meleshko T K, Sushchenko I G, Yakimansky A V, Pulyalina A Y, Toikka A M & Pientka Z, *J Appl Polym Sci*, 117 (2010) 2175.
35 Kavitha B, Prabakar K, Siva K, Srinivasu D, Srinivas C, Aswal V K, Siriguri V & Narsimlu V N, *IOSR J Appl Chem*, 2 (2012) 16.
36 Polotskaya G A, Pulyalina A Y, Goikhman M, Podeshvo I, Rostovtseva V, Shugurov S, Gofman I, Saprykina N, Gulii N, Loretsyan N & Toikka A, *Sci Rep*, 8 (2018) 1.

37 Munoz R C, Galiano F, Fila V, Drioli E & Figoli A, *Sep Purif Technol*, 199 (2018) 27.
38 Cheng X, Cai W, Chen X, Shia Z & Li J, *RSC Adv*, 9 (2019) 15457.
39 Suna D, Yang Q C, Suna H L, Liu J M, Xing Z L & Li B B, *Desalin Water Treat*, 57 (2016) 9123.
40 Roychowdhury S & Mitra D, *Environ Prog Sustain Energy*, 37 (2018) 1901.
41 Thermoset Polymers: Polyimide (Thomas Industry Update, New York) 2020 https://www.thomasnet.com/articles/plastics-rubber/thermoset-polyimide/ (Accessed on 20th April, 2020).
42 Eaton P, Quaresma P, Soares C, Neves C, Almeida M P, Pereira E & West P, *Ultramicroscopy*, 182 (2017) 179.
43 Jia W, Sun W, Xia C, Yang X, Cao Z & Zhang W, *RSC Adv*, 7 (2017) 54441.
44 Kwon Y S, Chaudhari S, Kim C E, Son D H, Park J H, Moon M J, Shon M Y, Park M Y & Nam S E, *RSC Adv*, 8 (2018) 20669.
45 Omara W, Amin R, Elhaes H, Ibrahim M & Elfeky S A, *Recent Pat on Nanotech*, 9 (2015) 195.
46 Wade L G, Singh M S, *Organic Chemistry* (Pearson Education: India, sixth edition) 2007, 264, ISBN-81-7758-739-0.
47 Ismail N H, Salleh W N W, Sazali N & Ismail A F, *Sep Sci Technol*, 52 (2017) 2137.
48 Goh P S, Ismail A F, Sanip S M,Kasim M A & Aziz M, *Sep Sci Technol*, 46 (2011) 1250.
49 Jain A, Dalai A K & Chaurasia S P, *Int J Res Sci Innov*, 4 (2017) 113.
50 Jyoti G, Keshav A & Anandkumar J, *J Eng*,(2015) doi:10.1155/2015/927068.
51 Azimi H, Thibault J & Tezel F H, *J Fluid Flow Heat Mass Transf*, 5 (2019) 53.
52 Jae J, Tompsett G A, Foster A J, Hammond K D, Auerbach S M, Lobo R F & Huber G W, *J Catal*, 279 (2011) 257.
53 Suda H & Haraya K, Chem Commun**,** (1997) doi:10.1039/A606385C .